Chen et al. EURASIP Journal on Wireless Communications and Networking (2015) 2015:237
DOI 10.1186/s13638-015-0468-1

EURASIP Journal on Wireless Communications and Networking
a SpringerOpen Journal

RESEARCH Open Access

Fisheye-lens-based space division multiplexing system for visible light communications

Te Chen[1,2], Lu Liu[1,2*], Zhong Zheng[1], Jie Song[1], Kai Wu[1] and Weiwei Hu[1*]

Abstract

This paper presents the high-diversity space division multiplexing (SDM) visible light communications (VLCs) utilizing a fisheye-lens-based imaging receiver. The receiver features ultra-wide field-of-view, good illumination uniformity, ultra-high imaging quality, and compact size; therefore, it can realize omnidirectional receiving and provide high spatial diversity for the SDM VLC system. In the presented system, four data streams are parallelly transmitted by commercial phosphorescent white light-emitting diodes, and discrete multitone signals based on quadrature amplitude modulation and bit loading are employed to achieve high spectral efficiency. The experiment verifies that the interchannel interference is effectively alleviated due to the high spatial diversity provided by the fisheye-lens-based receiver, and an aggregate data rate of 1.3 Gbit/s is achieved with the limited 3-dB bandwidth of 20 MHz. Besides, it is feasible to extend the system to more channels to achieve higher capacity. The experimental results indicate that the fisheye-lens-based imaging receiver is a potential candidate for high-speed VLC applications.

Keywords: Visible light communications, Space division multiplexing, Fisheye lens, Imaging receiver, Spatial diversity

1 Introduction

Nowadays, the radio frequency (RF) wireless communication technology has been widely used all around the world. However, as the data traffic exponentially increases in recent years, the wireless communication system has to be faced with a major challenge, which demands for additional bandwidth. Optical wireless communications turn out to be an alternative solution because of its advantages of free license, enhanced security, and high immunity to electromagnetic interference. Owing to the rapid improvement of solid-state lighting technology, visible light communication (VLC) based on white light-emitting diodes (LEDs), which can provide simultaneous illumination and data transmission, has drawn extensive interest over the past decade [1–4].

However, the realization of high-speed transmission is challenging due to the limited modulation bandwidth of the LEDs (several MHz). In order to improve the data rate, many approaches have been investigated, including filtering out the slow-response phosphorescent light [5], equalization [6], wavelength division multiplexing (WDM) [7], polarization division multiplexing (PDM) [8], high-efficiency modulation formats [9–11], and novel structures for high-bandwidth LEDs [12].

Spatial-multiplexing multiple input multiple output (MIMO) is another candidate to realize high-speed VLCs [13–17]. On the one hand, in order to achieve moderately uniform illumination, multiple LED lamps are usually employed, which can naturally serve as the transmitter array. On the other hand, the use of spatial-multiplexing technique enables high capacity without the need for additional power or bandwidth. However, since the channel gain is real and nonnegative, the VLC channels are highly correlated, and then the performance of the spatial-multiplexing system can be significantly degraded. In allusion to this problem, it has been

* Correspondence: luliu@pku.edu.cn; wwhu@pku.edu.cn
[1]State Key Laboratory of Advanced Optical Communication Systems and Networks, School of Electronics Engineering and Computer Science, Peking University, Beijing 100871, China
Full list of author information is available at the end of the article

indicated that by increasing the spacing of the receiving elements, adequate spatial diversity can be ensured [14]; nonetheless, it violates the demand for compact receiver. Another potential solution is to employ an imaging receiver [15], and the convex-lens-based imaging VLC systems were experimentally demonstrated in [16, 17]. However, the conventional imaging system could be impractical due to some major limitations. First, since the field-of-view (FOV) of the convex lens is small, the conventional imaging system can only work with small incidence angles (less than 10° as in [16, 17]). Besides, due to the poor imaging quality of the convex lens, the crosstalk between different channels is difficult to be eliminated. In addition, the size of the projected image is usually very large, so it cannot match the off-the-shelf small-sized detector array.

In order to solve these problems, we have proposed a novel imaging receiver scheme based on fisheye lens for spatial-multiplexing VLC applications [18], which features ultra-wide FOV, good illumination uniformity, ultra-high imaging quality, and compact size. Therefore, this receiver can function well even with large incidence angles, and it can provide high spatial diversity for demultiplexing of the optical signals. In this paper, we further demonstrate the proof of concept of a four-channel space division multiplexing (SDM) VLC system utilizing the fisheye-lens-based imaging receiver. In the demonstration, discrete multitone (DMT) signals with quadrature amplitude modulation (QAM) and bit loading are employed to achieve high spectral efficiency, and due to the high spatial diversity provided by the fisheye-lens, the interchannel interference is effectively alleviated. As this paper mainly focus on the verification of high spatial diversity of the SDM system, the circuits employed in the experiment are not fully optimized. Despite this, the data rate of 356.3, 312.5, 323.8, and 343.1 Mbit/s is achieved for the four SDM channels, respectively. Thus, an aggregate data rate of over 1.3 Gbit/s is realized with the 3-dB bandwidth of 20 MHz, while the bit error rates (BERs) for the four channels are below the forward error correction (FEC) threshold.

The remainder of this paper is organized as follows. In Section 2, we will present the proposed fisheye-lens-based imaging receiver scheme and its projection model. Following that, Section 3 will show the experimental setup and Section 4 will present the experimental results and discussions. The paper conclusion will be included in Section 5.

2 Proposed fisheye-lens-based imaging receiver for spatial-multiplexing VLCs

Figure 1 shows the schematic diagram of the fisheye-lens-based spatial-multiplexing VLC system and its projection model. In this system, the LED lamps provide indoor illumination and transmit parallel data streams. Instead of using the simple convex lens, a fisheye lens is employed as the imaging lens to project the incident light onto the receiving plane, and then the detector array receives the spatial-multiplexing signal. It should be noted that the fisheye lens, which is a bionic lens assembly that covers the hemispherical field, offers many advantages [19], including ultra-wide FOV (≥180°), good illumination uniformity, and ultra-high imaging quality. Therefore, the fisheye-lens-based receiver can realize omnidirectional receiving, and it can clearly separate the spatial-multiplexing signals from different LEDs, providing high spatial diversity.

The projection model of the receiver can be determined by using the polynomial projection function [18]. Assuming that a Lambertian LED is placed at $\boldsymbol{p}$ (r, θ, ϕ) with a distance of r to the fisheye lens, then, with the channel DC gain on the direct path $H_d(0)$ and the reflected path $dH_{\mathrm{ref}}(0)$ as defined in [1, 18], the received optical power is defined as

$$P_r = P_t\left[H_d(0) + \int_{\mathrm{walls}} dH_{\mathrm{ref}}(0)\right] \tag{1}$$

where P_t is the transmitted optical power. Since the fisheye lens has ultra-high imaging quality, the projected light is focused onto a single dot $\boldsymbol{p}'(\rho', \phi)$ on the focal plane, whose coordinate is given by [18]

$$\rho' = k_1\theta + k_2\theta^2 + k_3\theta^3 + k_4\theta^4 + k_5\theta^5 \ (\mathrm{m}) \tag{2}$$

where k_i is the ith order coefficient and θ is the incident angle to the receiver. In order to avoid the total optical power falling onto the blind areas between the adjacent elements of the receiver array, the receiving plane is assumed to be fixed beyond the focal plane with an off-focus distance of l [18]; thus, the light is defocused, and the optical power received at arbitrary point $\boldsymbol{p}''(\rho'', \phi)$ on the receiving plane is given by [18]

$$dP_r' = \begin{cases} P_r \dfrac{dA''}{2\pi r''^2\left[1-\cos\left(\psi_{1/2}\right)\right]}, & \psi \le \psi_{1/2} \\ 0, & \psi > \psi_{1/2} \end{cases} \tag{3}$$

where dA'' is the unit area at $\boldsymbol{p}''$, r'' is the distance from $\boldsymbol{p}'$ to $\boldsymbol{p}''$, $\psi_{1/2} = \arctan(D / 2f)$ is the half divergence angle, and ψ is the angle from $\mathrm{p}'\bar{\mathrm{p}}''$ to the optical axis. Then, by integrating the optical power, the received optical power over the detector can be determined:

$$P_r' = \int_{\mathrm{Detector}} dP_r' \tag{4}$$

With the polynomial projection model, we will briefly analyze the projected image and the channel matrix of the spatial-multiplexing VLC system. In the following

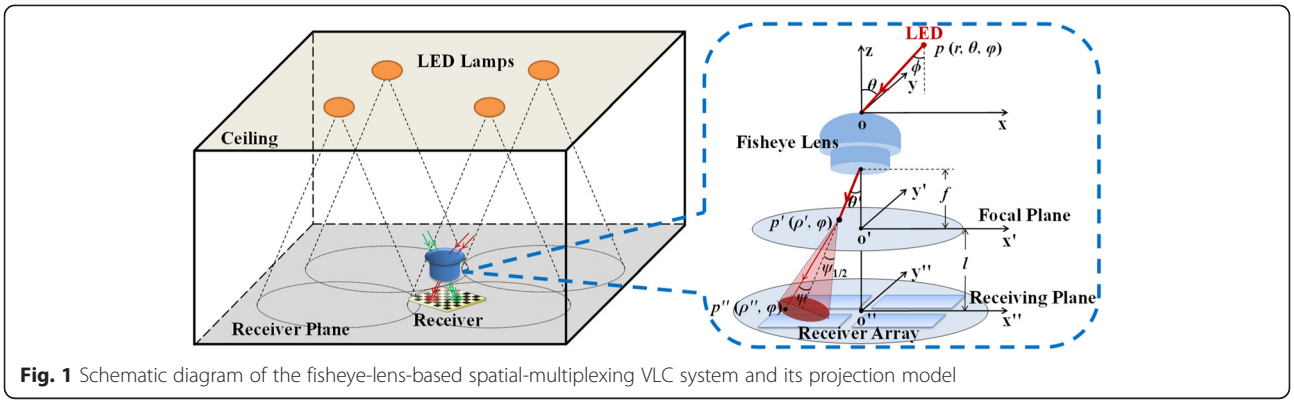

Fig. 1 Schematic diagram of the fisheye-lens-based spatial-multiplexing VLC system and its projection model

simulation, a commercial fisheye lens, as analyzed in [18], is employed. The fisheye-lens-based receiver is assumed to locate on the center of the floor of the room, measuring 5 m × 5 m × 2.5 m [1, 18]. Four LED (semiangle of 65°) transmitters (Txs) are symmetrically mounted on the ceiling with the distance of 1 m to the neighboring walls. Then, given the following parameters: the optical transmittance of 0.9, the area of the entrance pupil of 0.5 cm^2, $l = 1.3$ mm, and the wall reflectivity of 0.7, the normalized optical intensity on the receiving plane is obtained, which is shown in Fig. 2. The simulation result indicates that the fisheye lens can effectively separate the images of the LEDs, offering high spatial diversity for the spatial-multiplexing VLCs. Note that although we only present the simulation in which the receiver is placed on the center, it has been investigated that high spatial diversity can be always obtained with various positions under indoor environment [18]. In addition, the projected image is planar and small in size (<1 cm^2), so it can match the compact detector array. By integrating the fisheye lens with the detector array, high reliability can be guaranteed.

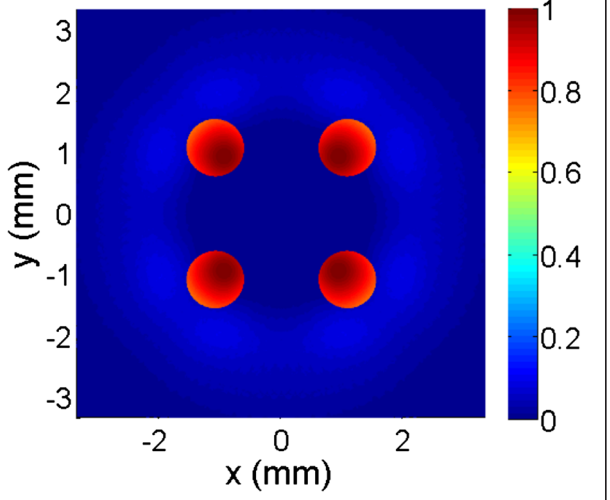

Fig. 2 Normalized optical intensity on the receiving plane

Consider that there are four detectors covering the four quadrants of the receiving plane, the channel matrix can be calculated by integrating the optical power due to each LED over each detector, given by

$$\mathbf{H} = \begin{bmatrix} 1.459 & 0.063 & 0.063 & 0.037 \\ 0.063 & 1.459 & 0.037 & 0.063 \\ 0.063 & 0.037 & 1.459 & 0.063 \\ 0.037 & 0.063 & 0.063 & 1.459 \end{bmatrix} \times 10^{-6} \quad (5)$$

where $\mathbf{H}(i,j)$ is the channel gain between the ith detector and the jth LED. We can see that in each row or column, there is an element that is much greater than the others, which means that a low correlation of the four channels is achieved, and that the interference between different channels is effectively eliminated. Therefore, high-performance SDM VLC applications can be potentially realized.

3 Experimental setup

The block diagram and experimental setup of the fisheye-lens-based SDM VLC system is shown in Fig. 3, together with the projected image of the LED Txs, which is in accordance with the simulation result. In order to match the scenarios where four LED lamps are installed on the ceiling [1, 18], a cuboid shelf was employed to imitate a room. As the Tx array, four commercial phosphorescent white LEDs (OSTAR) were symmetrically mounted on the ceiling of the shelf, with the distance between adjacent LEDs of 40 cm. The LED module provides a luminous flux of ~250 lm at 700 mA dc, and its full viewing angle at half power is 130°. In order to drive all the four channels simultaneously, four independent signals were generated by software before feeding into the arbitrary waveform generator (AWG, Tektronix), and then, the LEDs were modulated by the output signals of the AWGs superimposed on a DC current of 700 mA via bias-T.

The fisheye-lens-based imaging receiver, which mainly consisted of a commercial fisheye lens (16 mm F/2.8, FOV

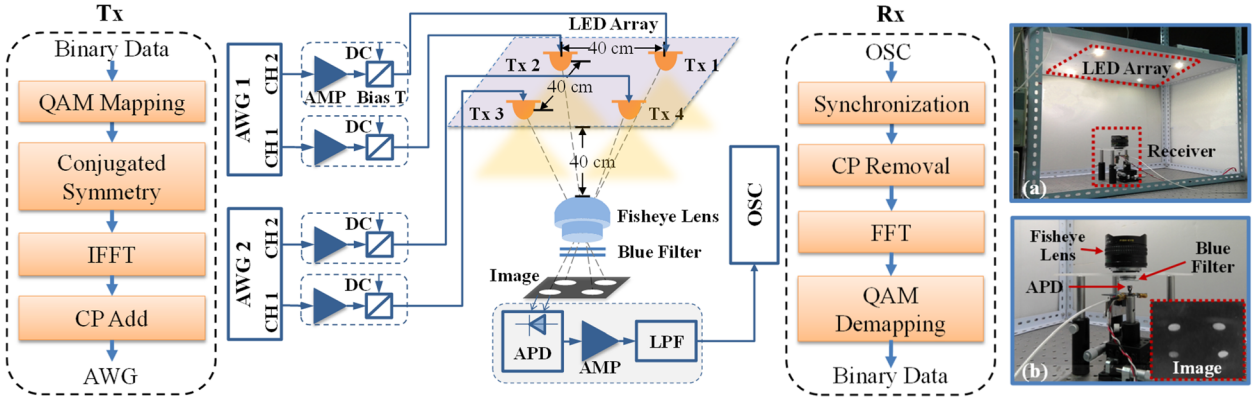

Fig. 3 Block diagram and experimental setup of the fisheye-lens-based SDM VLC system. **a** Overall system. **b** Fisheye-lens-based imaging receiver and the projected image. *AWG* arbitrary waveform generator, *OSC* real-time oscilloscope, *AMP* amplifier, *LPF* low-pass filter, *APD* avalanche photodiode, *CP* cyclic prefix

of 180°), a blue filter, and an avalanche photodiode (APD) module, was fixed on the center of the floor with a vertical distance of 40 cm to the ceiling (note that the distance between the Tx and the fisheye-lens-based receiver was larger than 40 cm). In this case, the illuminance level of around 1000 lx was obtained in front of the receiver, which was within the lighting standard for the working environment [1], and the typical indoor distance of several meters could be achieved by using more LED modules in parallel. Moreover, the experimental setup was in accordance with the scenarios in [1, 18], and the incidence angle to the imaging receiver was 35.3°, which was much larger than that of the previous works [16, 17]. In lack of an APD array, a single APD module (responsivity of 0.42 A/W at 620 nm, bandwidth of 80 MHz, and active area of 7.1 mm^2) was employed in the verification experiment. Since the signals from different LEDs can be always clearly separated over individual quadrants of the imaging plane [18], we simply adjusted the position of the APD and placed it on the corresponding quadrant to receive the optical signal under test. In this way, all the four SDM channels were tested individually to verify the high spatial diversity. The received signal was then recorded by a real-time oscilloscope (OSC, Tektronix) for further off-line signal processing.

In the experiment, QAM-based DMT signals were employed, which consisted of N subcarriers within the bandwidth of B ($N = 64$, $B = 50$ MHz, and $N = 128$, $B = 80$ MHz for two cases, respectively, which will be presented in the following section). The first subcarrier corresponding to DC was left unmodulated, and when measuring the transmission performance of the SDM system, manual bit loading was applied on the other subcarriers to adapt to the channel quality. As a result, the spectral efficiency could be enhanced. After being recorded by the OSC, the signals were demodulated according to the bit-loading mask, and then the BERs were calculated for each subcarrier.

4 Experimental results and discussions

Before transmission performance assessment of the fisheye-lens-based SDM system, the frequency characteristic of the electro-optical-electrical (EOE) channel was firstly measured, and Fig. 4 illustrates the normalized EOE channel responses for all the four SDM channels. It can be seen that the four channels have similar frequency characteristics with the 3-dB EOE bandwidth around 20 MHz. Note that since the APD itself has a relatively larger bandwidth, it can be concluded that the EOE bandwidth is mainly limited by the LED module.

In order to verify that high spatial diversity can be obtained and that the interchannel interference can be effectively alleviated, we compared the BER performance in the two cases where (i) only one Tx was operational with the other three LEDs illuminating and (ii) all the four SDM channels were operational simultaneously to transmit different signals. In the measurement, QAM-based DMT signals were employed, which consisted of

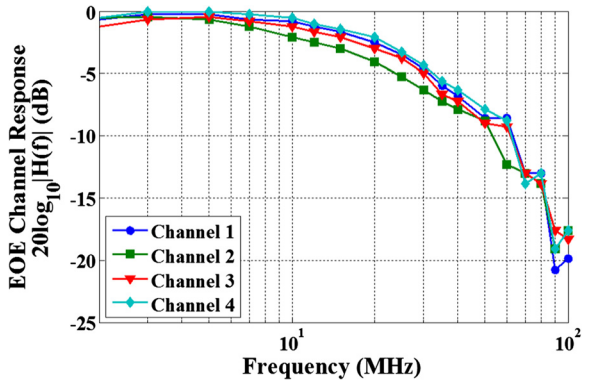

Fig. 4 Normalized EOE channel responses of the SDM channels

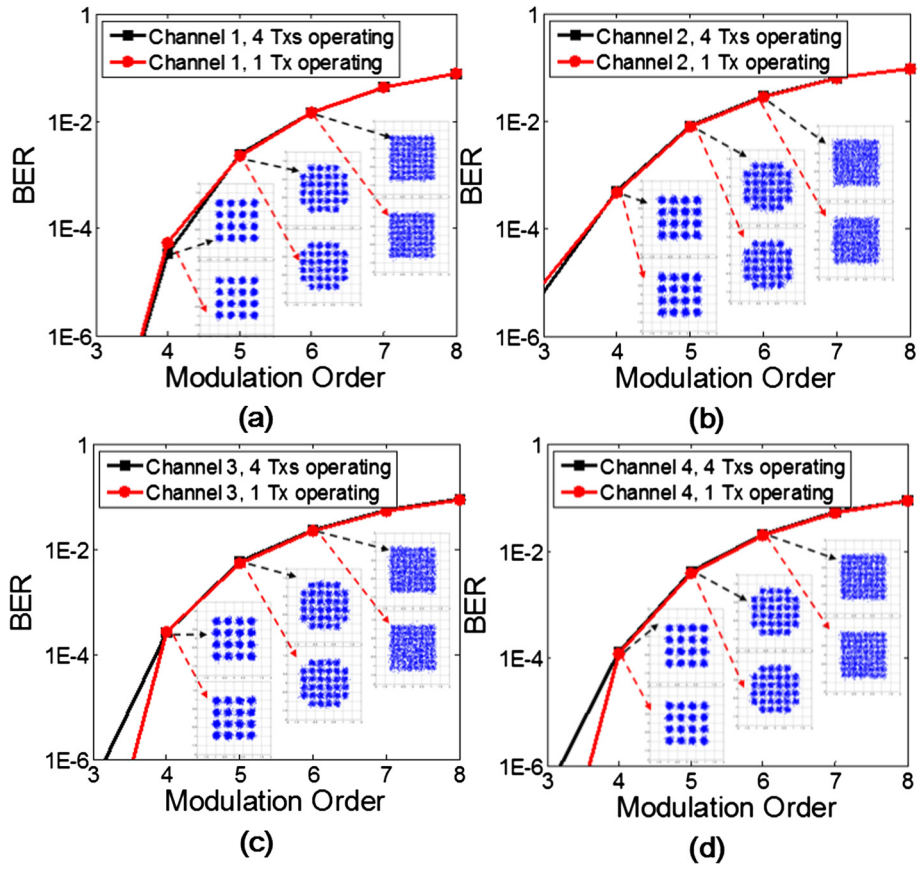

Fig. 5 BER performance as a function of the modulation order together with the constellation diagrams of the received data. **a** Channel 1. **b** Channel 2. **c** Channel 3. **d** Channel 4

64 subcarriers within the baseband bandwidth of 50 MHz, and uniform modulation orders were applied on all the 63 (without DC) subcarriers. Figure 5 illustrates the resultant BERs as a function of the modulation order for all the four SDM channels together with the constellation diagrams of the received data. From this figure, we can find that the BER performance is not significantly degraded when four Txs are operational at the same time, which means that the crosstalk between different SDM channels is efficiently eliminated by using the high-spatial-diversity imaging receiver.

Finally, we measured the transmission performance of the fisheye-lens-based SDM VLC system. In the measurement, the baseband bandwidth was set to 80 MHz, which was equal to the bandwidth of the APD module, and the QAM-based DMT signals consisted of 128 subcarriers (the carrier spacing was 0.625 MHz). Since the bandwidth of the DMT signals exceeded the 3-dB EOE bandwidth of the SDM channels, the signal-to-noise ratio (SNR) could be significantly degraded over the high-order subcarriers. In order to solve this problem, we manually adjusted the modulation orders on different subcarriers to adapt to the channel quality [20]. In this way, the transmission rate was enhanced, while the total BER was kept below the threshold of 3.8×10^{-3} that can be compensated by the FEC coding.

Figure 6 shows the bit loading masks of all the four SDM channels. Due to the imperfection of the driving circuits, the spectral efficiencies on the first couple of subcarriers are degraded, and different channels have different bit loading masks despite the symmetrical experimental setup. Besides, as the frequency increases, the bit distribution decreases since the SNR is degraded.

The resultant BER performance on different subcarriers is illustrated in Fig. 7 together with the constellation diagrams on different subcarriers. It can be seen that within a group of subcarriers of the same modulation order, the BER increases with the frequency. However, the BERs vary significantly over some high-order (beyond ~100th) subcarriers even though they have the same modulation order. This can be explained that since these subcarriers are far beyond the 3-dB EOE bandwidth (over −10 dB), the SNR is severely degraded. The resultant BERs of the four SDM channels are 3.0×10^{-3}, 2.6×10^{-3}, 2.7×10^{-3}, and 3.2×10^{-3}, respectively, which are all below the FEC limit. With the bit-loading masks

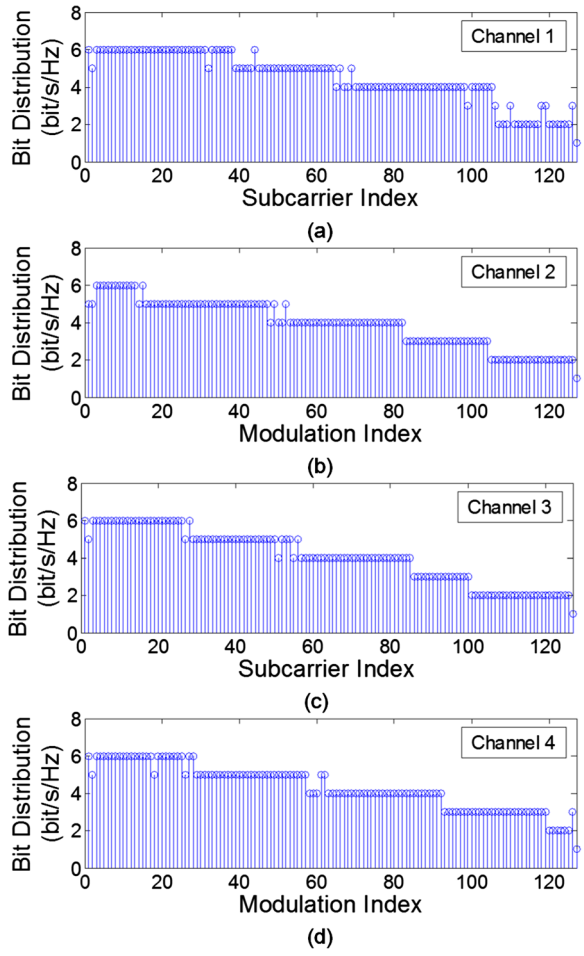

Fig. 6 Bit loading masks. **a** Channel 1. **b** Channel 2. **c** Channel 3. **d** Channel 4

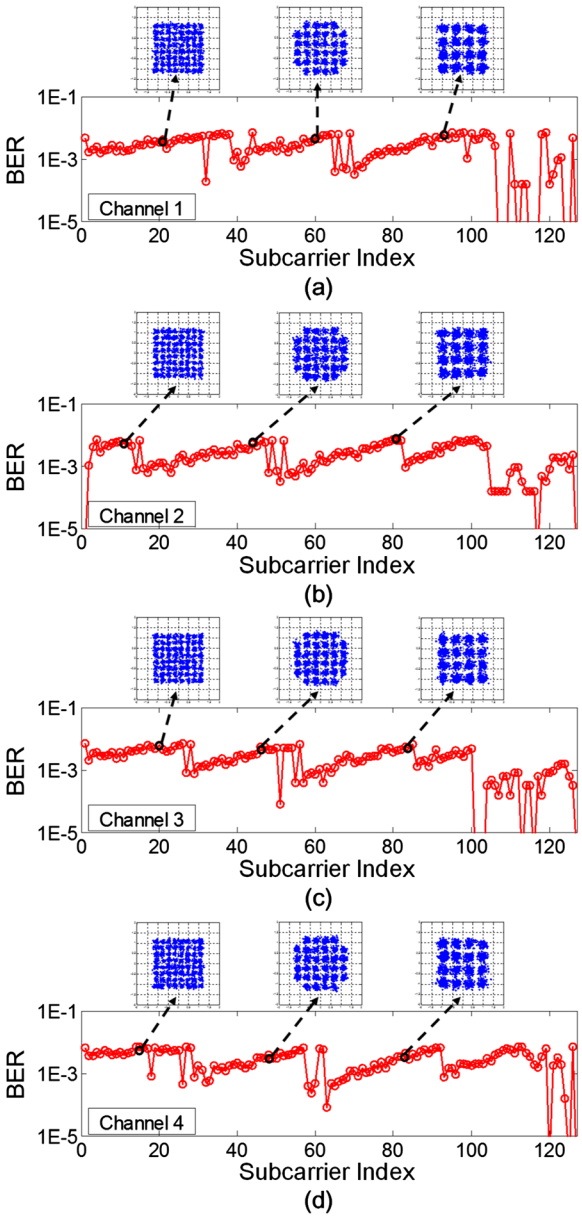

Fig. 7 BER performance on different subcarriers. Together with the constellation diagrams on different subcarriers. **a** Channel 1. **b** Channel 2. **c** Channel 3. **d** Channel 4

as shown in Fig. 6, the transmission rate for the four channels are 356.3, 312.5, 323.8, and 343.1 Mbit/s, respectively, leading to an aggregate rate of over 1.3 Gbit/s. Note that since we mainly focus on the verification of high spatial diversity in this work, the circuits employed in the demonstration were not fully optimized. With further optimization of the circuits, it is potential to achieve better transmission performance.

Finally, it should be noted that although the demonstrated SDM VLC system consists of only four SDM channels, it is feasible to be extended to more channels since the optical signals from different channels can be always clearly separated by the fisheye lens. As a result, it is potential to further multiply the system capacity by utilizing more LEDs for high-speed parallel transmissions. In addition, for practical application, a detector array integrated with the fisheye lens should be employed to receive the SDM signals, and misalignment between the projected image and the element of the detector array could happen, especially in the scenarios with moving or random-positioned receivers. In this case, the SDM scheme will become a typical spatial-multiplexing MIMO system as shown in our previous work [18], and with the MIMO demultiplexing process, the signal can be recovered. It has been indicated that the fisheye-lens-based imaging receiver scheme has superior performance on demultiplexing of the MIMO signals, and it can potentially realize high-speed parallel transmissions with little interchannel interference [18]. The detailed experimental analysis of the fisheye-lens-based MIMO VLC transmission will be left for a future study.

5 Conclusions

In conclusion, this paper has presented the high-diversity fisheye-lens-based VLC system, which can realize high-performance SDM transmission because of the advantages of ultra-wide FOV, good illumination uniformity, ultra-high imaging quality, and compact size. By using the polynomial projection model, the optical intensity on the receiving plane was obtained, showing that low correlation of the SDM channels was achieved. In the experimental demonstration, the system consisted of a four-channel SDM link with the 3-dB EOE bandwidth of around 20 MHz. In order to achieve high spectral efficiency, QAM-based DMT signals with bit-loading were employed, and four commercial phosphorescent white LEDs were utilized to transmit parallel data streams. The experiment results indicated that the BER performance was not significantly degraded when four Txs were operational at the same time, which verified that the crosstalk between different SDM channels was effectively alleviated due to the high spatial diversity provided by the fisheye-lens-based imaging receiver. Besides, the transmission rate of 356.3, 312.5, 323.8, and 343.1 Mbit/s was achieved for the four channels, respectively, while the BERs were below the FEC threshold, leading to an aggregate data rate of over 1.3 Gbit/s. In addition, since the optical signals from different channels can be always clearly separated by the fisheye lens, it is feasible to extend the SDM system to more channels to achieve higher capacity. The demonstration indicated that the fisheye-lens-based imaging receiver is a potential candidate for high-speed VLC applications.

Abbreviations

AMP: amplifier; APD: avalanche photodiode; AWG: arbitrary waveform generator; BER: bit error rate; CP: cyclic prefix; DMT: discrete multitone; EOE: electro-optical-electrical; FEC: forward error correction; FOV: field-of-view; LED: light-emitting diode; LPF: low-pass filter; MIMO: multiple input multiple output; OSC: oscilloscope; PDM: polarization division multiplexing; QAM: quadrature amplitude modulation; RF: radio frequency; SDM: space division multiplexing; SNR: signal-to-noise ratio; Tx: transmitter; VLC: visible light communication; WDM: wavelength division multiplexing.

Competing interests

The authors declare that they have no competing interests.

Acknowledgements

This work was partially supported by the National Natural Science Foundation of China under Grant 61320106001, the National High Technology Research and Development Program of China under Grants 2013AA013602 and 2013AA013603, the Science and Technology on Information Transmission and Dissemination in Communication Networks Laboratory under Grant ITD-U14011/KX142600018, the Specialized Research Fund for the Doctoral Program of Higher Education under Grant 20120001110094, and the State Key Laboratory of Advanced Optical Communication Systems and Networks, China.

Author details

[1]State Key Laboratory of Advanced Optical Communication Systems and Networks, School of Electronics Engineering and Computer Science, Peking University, Beijing 100871, China. [2]Science and Technology on Information Transmission and Dissemination in Communication Networks Laboratory, Shijiazhuang 050081, China.

Received: 25 May 2015 Accepted: 19 October 2015
Published online: 29 October 2015

References

1. T Komine, M Nakagawa, Fundamental analysis for visible-light communication system using LED lights. IEEE Trans. Consum. Electron. **50**(1), 100–107 (2004)
2. H Le Minh, Z Ghassemlooy, D O'Brien, G Faulkner, Indoor gigabit optical wireless communications: challenges and possibilities, in *Proceedings of ICTON* (IEEE, Munich, 2010)
3. DK Borah, AC Boucouvalas, CC Davis, S Hranilovic, K Yiannopoulos, A review of communication-oriented optical wireless systems. EURASIP J. Wirel. Commun. Netw. **2012**(1), 1–28 (2012)
4. H Haas, Visible light communications, in *Proceedings of OFC* (IEEE/OSA, Los Angeles, 2015)
5. SW Wang, F Chen, L Liang, S He, Y Wang, X Chen, W Lu, A high-performance blue filter for a white-led-based visible light communication system. IEEE Wirel. Commun. **22**(2), 61–67 (2015)
6. H Li, X Chen, J Guo, H Chen, A 550 Mbit/s real-time visible light communication system based on phosphorescent white light LED for practical high-speed low-complexity application. Opt. Express **22**(22), 27203–27213 (2014)
7. G Cossu, AM Khalid, P Choudhury, R Corsini, E Ciaramella, 3.4 Gbit/s visible optical wireless transmission based on RGB LED. Opt. Express **20**(26), B501–B506 (2012)
8. Y Wang, C Yang, Y Wang, N Chi, Gigabit polarization division multiplexing in visible light communication. Opt. Lett. **39**(7), 1823–1826 (2014)
9. N Chi, Y Wang, Y Wang, X Huang, X Lu, Ultra-high-speed single red-green-blue light-emitting diode-based visible light communication system utilizing advanced modulation formats. Chin. Opt. Lett. **12**(1), 010605 (2014)
10. MA Kashani, M Kavehrad, On the performance of single- and multi-carrier modulation schemes for indoor visible light communication systems, in *Proceedings of Globecom* (IEEE, Austin, 2014)
11. PA Haigh, ST Le, S Zvanovec, Z Ghassemlooy, P Luo, T Xu, P Chvojka, T Kanesan, E Giacoumidis, P Canyelles-Pericas, H Le Minh, W Popoola, S Rajbhandari, I Papakonstantinou, I Darwazeh, Multi-band carrier-less amplitude and phase modulation for bandlimited visible light communications systems. IEEE Wirel. Commun. **22**(2), 46–53 (2015)
12. D Tsonev, H Chun, S Rajbhandari, JJD McKendry, S Videv, E Gu, M Haji, S Watson, AE Kelly, G Faulkner, MD Dawson, H Haas, D O'Brien, A 3-Gb/s single-LED OFDM-based wireless VLC link using a gallium nitride μLED. IEEE Photonics Technol. Lett. **26**(7), 637–640 (2014)
13. T Fath, H Haas, Performance comparison of MIMO techniques for optical wireless communications in indoor environments. IEEE Trans. Commun. **61**(2), 733–742 (2013)
14. A Burton, H Le Minh, Z Ghassemlooy, E Bentley, C Botella, Experimental demonstration of 50-Mbps visible light communications using 4 × 4 MIMO. IEEE Photonics Technol. Lett. **26**(9), 945–948 (2014)
15. L Zeng, D O'Brien, H Le Minh, G Faulkner, K Lee, D Jung, Y Oh, ET Won, High data rate multiple input multiple output (MIMO) optical wireless communications using white LED lighting. IEEE J. Sel. Areas Commun. **27**(9), 1654–1662 (2009)
16. KD Dambul, D O'Brien, G Faulkner, Indoor optical wireless MIMO system with an imaging receiver. IEEE Photonics Technol. Lett. **23**(2), 97–99 (2011)
17. AH Azhar, T Tran, D O'Brien, A Gigabits indoor wireless transmission using MIMO-OFDM visible-light communications. IEEE Photonics Technol. Lett. **25**(2), 171–174 (2013)
18. T Chen, L Liu, B Tu, Z Zheng, W Hu, High-spatial-diversity imaging receiver using fisheye lens for indoor MIMO VLCs. IEEE Photonics Technol. Lett. **26**(22), 2260–2263 (2014)
19. K Miyamoto, Fish eye lens. J. Opt. Soc. Amer. **54**(8), 1060–1061 (1964)
20. J Vucic, C Kottke, S Nerreter, A Buttner, KD Langer, J Walewski, White light wireless transmission at 200 Mb/s net data rate by use of discrete-multitone modulation. IEEE Photonics Technol. Lett. **21**(20), 1511–1513 (2009)